01,16

Optical and dielectric characteristics of semimetallic compounds $Y_xLa_{1-x}Bi$ ($0 \leq x \leq 1$)

© Yu.V. Knyazev, Yu.I. Kuz'min

M.N. Mikheev Institute of Metal Physics, Ural Branch, Russian Academy of Sciences, Yekaterinburg, Russia

E-mail: knyazev@imp.uran.ru

Received March 29, 2024
Revised March 29, 2024
Accepted March 31, 2024

The results of experimental studies of the optical and dielectric properties of cubic compounds $Y_xLa_{1-x}Bi$ are presented. In the spectral range $0.22-15\,\mu$m, the refractive indices and absorption coefficients were measured ellipsometrically, using which the energy dependences of the dielectric constant, reflectivity, optical conductivity and the function of characteristic electron losses were calculated. The features of quantum light absorption are interpreted on the basis of a comparative analysis of experimental and theoretical optical conductivity spectra. The anomalous behavior of spectral characteristics in the infrared range of the spectrum confirms the semi-metallic nature of the compounds

Keywords: optical properties, dielectric functions, optical conductivity, intermetallic compounds, electronic structure.

DOI: 10.61011/PSS.2024.05.58489.71

1. Introduction

Intermetallic binary rare earth compounds with V group *p*-metals (monopnictides) with a variety of structural, electric and magnetic properties have been extensively studied over recent years. A large amount of materials whose physical properties vary within a wide range from semiconductor to metallic has been synthesized and studied (see [1]). Various types of magnetic ordering were found in these compounds [2,3], and their electronic and crystal properties are sensitive to high pressure [4,5], substitution impurities [6,7] and stoichiometry variation [8,9]. Practical application prospects of REM monopnictides are associated with properties such as giant magnetoresistance [10,11], superconductivity [12], high magnetocaloric [13] and magnetooptic [14,15] effects. Features of electronic structure of such compounds allow them to be used as materials for optoelectronic devices [16,17].

This group of materials is represented by binary nonmagnetic YBi and LaBi compounds having NaCl type cubic lattice that transits, to a CsCl type tetragonal structure at high pressures of 23 and 11.5 GPa, accordingly. Volumetric collapse in such transition achieves 5% (YBi) and 8.9% (LaBi) [18,19]. Few experimental studies showed that features of the temperature dependences of transport properties of these compounds are explained by a semimetallic type of conductivity and low concentration of current carriers [20,21]. Both materials exhibit extremely high magnetoresistance that achieves about 10^5% at low temperatures as well as hopping transition to superconducting state induced by high pressure [22,23].

For YBi and LaBi compounds, band spectra were calculated using various computational schemes that showed that the structure of electronic states had some features near the Fermi energy E_F [24–27]. The one of the main features is a deep gap at E_F in densities of states of both compounds that explains their semimetallic properties and high thermoelectric capability. Theoretical studies [28–31] analyze the variation of structural, thermodynamic and mechanical properties of these compounds when exposed to temperature and hydrostatic pressure. Recent calculations [32,33], magnetic and photoemission research [34–36] have shown that these materials have three-dimensional topological semimetal properties. Their common feature is in that the band structure contains anomalous points whose valence band contacts the conduction band. Such situation induces a wide range of new physical phenomena related to volumetric and surface properties.

Doping of these binary intermetallic compounds with other elements has a considerable effect on their crystalline, electronic and thermodynamic properties [37,38]. Directional modifications of physical properties that occur when an impurity is introduced may be used for optimization of functional performance of these materials. According to the calculations [37], partial substitution of yttrium by lanthanum atoms in YBi considerably modifies the band spectrum of this compound, density of electronic states, structural, mechanical and thermodynamic parameters. Additional information on the features of energy band evolution in ternary $Y_xLa_{1-x}Bi$ may be obtained from spectral investigations. This study investigates optical and dielectric properties of this system to obtain the data on their concentration dependence and correlation with electronic

restructuring. Investigations were performed in a wide wavelength range, including IR, visible and UV bands.

2. Experiment

The studied polycrystalline $Y_xLa_{1-x}Bi$ ($x = 0, 0.25, 0.5, 0.75, 1$) samples were prepared by arc melting of stoichiometric proportions of high-purity metals ($\sim 99.99\%$) in pure argon atmosphere. The arc-melted ingots were annealed in vacuum 10^{-5} mm · Hg at $\sim 800^\circ$C during 10 h. X-ray analysis of powder samples performed in CuK_α-radiation using DRON-6 diffractometer confirmed that NaCl type cubic structure has formed in all alloys under study. For binary YBi and LaBi, lattice parameter values are close to those published before [25,26] and are equal to $a = 6.238$ and 6.570 Å. In ternary alloys with $x = 0.25$, 0.5 and 0.75, the lattice parameter gradually decreases taking on the values $a = 6.489$, 6.404 and 6.322 Å respectively.

Flat mirror surfaces of samples required for the optical experiment were ground and then polished on diamond pastes with various grain size. Optical constants — refraction and absorption indices were measured with accuracy 2–4% within the wavelength range $\lambda = 0.22-15\,\mu$m ($E = 0.083-5.64$ eV) by the Beattie ellipsometric method based on the measurement of amplitudes and phase shifts of reflected light waves s- and p-polarizations. Optical constants were used to calculate the real $\varepsilon_1(E)$ and imaginary $\varepsilon_2(E)$ parts of complex permittivity, reflectivity $R(E)$ and optical conductivity $\sigma(E) = \varepsilon_2\omega/4\pi$ (ω is the light wave frequency).

3. Results and discussion

Dispersion dependences $\varepsilon_1(E)$, $\varepsilon_2(E)$ and $R(E)$ of the compounds under consideration are shown in Figure 1. Behavior of these parameters with photon energy variation is generally specific to metallic media. This is indicated by negative values of ε_1 throughout the frequency range and by spectra division into intraband and interband optical absorption regions that is specific to conducting materials. At the same time, low values of R and $|\varepsilon_1|$ in the IR band indicate that metallic properties of these compounds degrade compared with good metals whose reflectivity approaches 1 and $|\varepsilon_1|$ is two to three orders of magnitude higher [39]. All curves shown in Figure 1 feature wide structures whose origin is associated with interband light absorption. Energy position and intensity of these features depend considerably on the impurity concentration which is reflected in transformation of the form of the shown spectra. Growth of yttrium atom content results in the shift of peaks towards the high-energy area with simultaneous reduction of their height which is very clearly exhibited in $\varepsilon_2(E)$ and $R(E)$.

Spectral dependences of optical conductivity of the $Y_xLa_{1-x}Bi$ compounds family under study are shown in Figure 2 (curves are shifted with respect to each other on

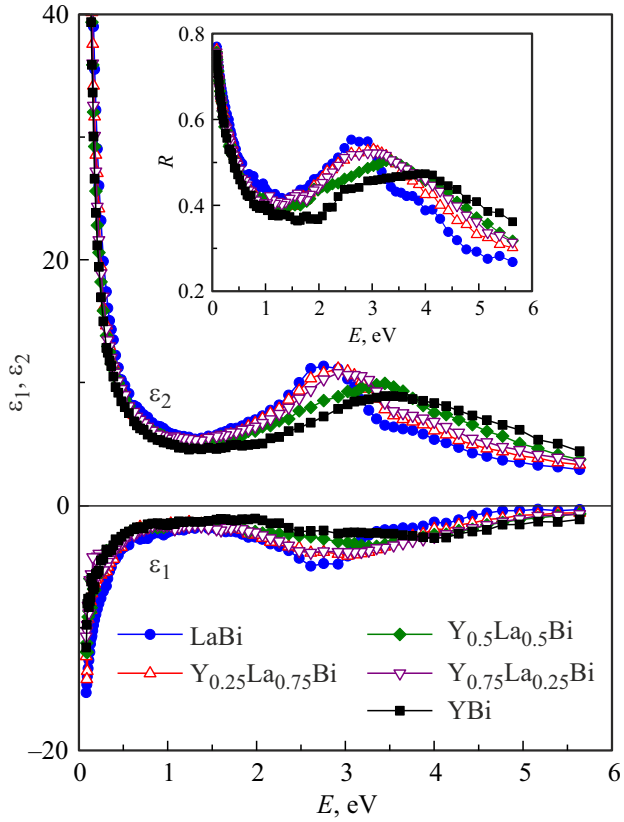

Figure 1. Dielectric functions $\varepsilon_1(E)$ and $\varepsilon_2(E)$ and reflectivity $R(E)$ of $Y_xLa_{1-x}Bi$.

the y-axis by 20 units). At energies higher than ~ 1 eV, dispersion behavior of all curves is defined by quantum absorption of light as shown by the intensive absorption bands whose spectral profile varies significantly according to the compound composition. When $\sigma(E)$ of binary intermetallic YBi (upper curve) has one wide band with its peak near 4 eV, then its shape varies considerably as lanthanum content grows. A new structure occurs on the high-energy slope of the band — a „shoulder" that transits to another less intensive peak as x decreases. Localization of the main peak gradually moves into the low-energy area and becomes equal to 2.9 eV for binary LaBi. In the long-wavelength region, values of $\sigma(E)$ are quite low and their slow growth is observed only at energies below ~ 0.3 eV. Such behavior of optical conductivity differs drastically from the Drude dependence $\sigma \sim 1/\omega^2$ specific to metallic materials and usually occurring below ~ 1 eV [39]. Such abnormal course of dispersion $\sigma(E)$ in the IR band has been observed earlier in compounds where the density of electronic states features a deep decline at the Fermi level [40,41].

Features of the frequency dependences of optical conductivity of intermetallic $Y_xLa_{1-x}Bi$ observed experimentally may be explained qualitatively based on the electronic spectra calculations performed in [37]. The calculations have shown that within $-10 < E_F < 10$ eV, Y $4d$, $5p$,

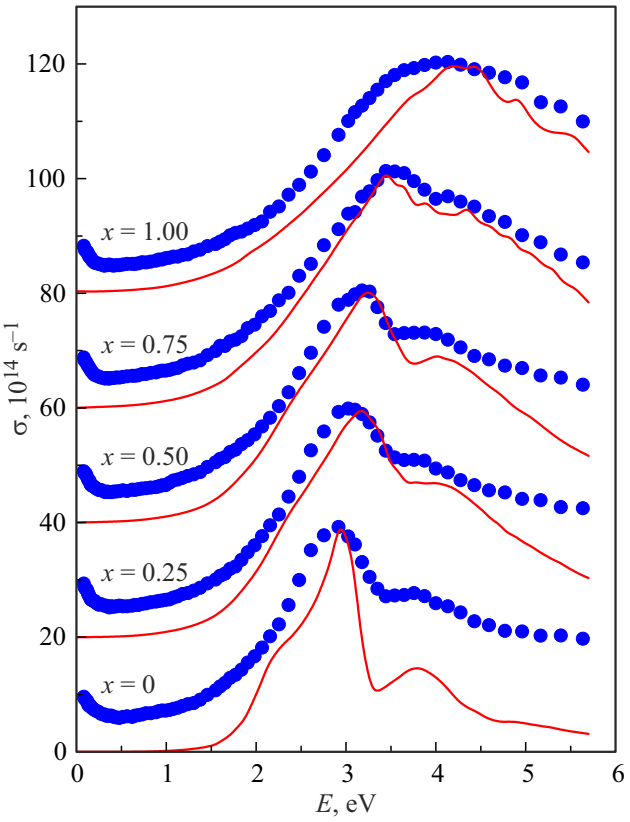

Figure 2. Optical conductance of $Y_xLa_{1-x}Bi$. Circles — experiment, solid lines — calculation from density of states [37]. The curves are shifted with respect to each other along the y-axis by 20 units.

La $5d, 6p, 4f$, Bi $6p$-bands dominate in the densities of electronic states $N(E)$ of all compounds. And several intensive peaks are formed due to these bands below and above the Fermi level. d-bans have high partial densities on both sides of E_F, while p-bands have high partial densities only at energies below E_F. In ternary intermetallic compounds as well as in LaBi narrow intensive peaks $N(E)$ associated with La $4f$-bands are localized within 1.4–1.7 eV above E_F. In all compounds, partial contributions of s-states are low and distributed over a wide energy region. Calculations of full and partial $N(E)$ show that a deep decline ~ 2 eV in width is present and included the Fermi level. This feature in the densities of states of binary YBi and LaBi is the cause of low concentration of conduction electrons and high electrical resistance of these materials [20–23]. Abnormally low values of the experimental optical conductivity observed in the low-energy spectrum range also correspond to $N(E)$ pattern shown in [37] and indicate degradation of metallic properties in the compounds under cosideration.

Modification of $\sigma(E)$ spectra in the quantum light absorption region is caused by successive electronic restructuring of the compounds during partial substitution of lanthanum atoms by yttrium atoms [37]. The most considerable changes in the electronic density of states occur above the Fermi level within 1–4 eV, where $N(E)$ structure is defined by hybridized d- and f-bands of the atoms of these elements. As the lanthanum content increases, the density of d-states varies just a little, while the intensity of the peak associated with $4f$-state increases considerably. It is interesting to compare the experimental optical conductivity spectra with the corresponding dependences calculated from the densities of states reported in [37]. Interband optical conductances of all compounds were calculated using the method proposed in [42] in accordance with convolutions of full $N(E)$ below and above E_F on the assumption of equal probability of all types of electronic transitions. These calculated data are shown in arbitrary

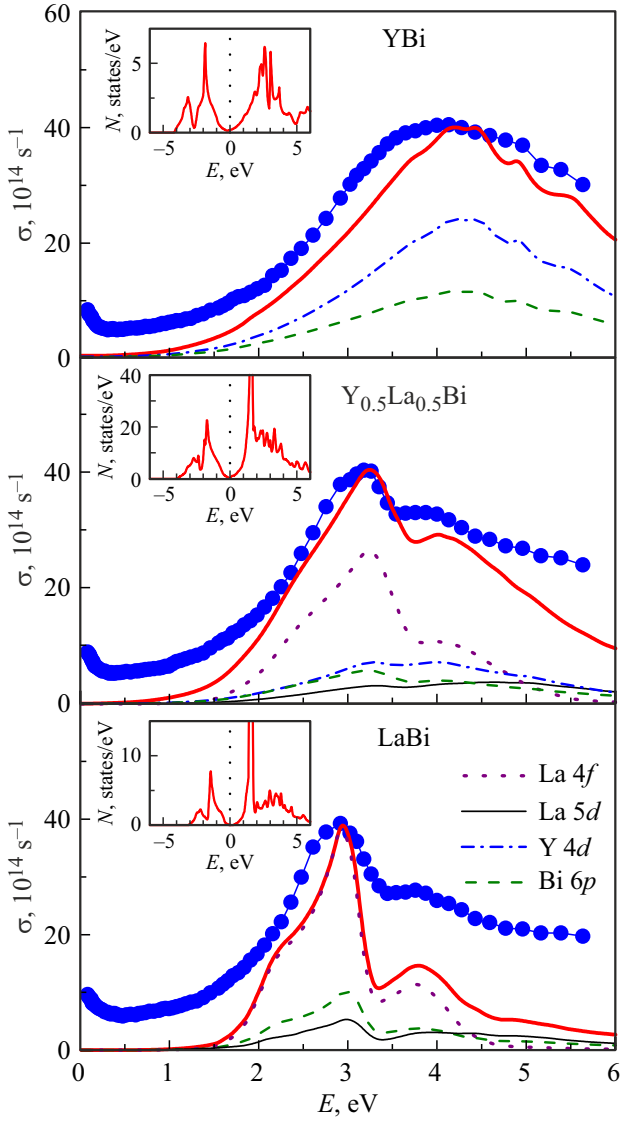

Figure 3. experimental (circles) and calculated (thick solid lines) energy dependences of optical conductivity of YBi, $Y_{0.5}La_{0.5}Bi$ and LaBi. Partial contribution from interband transitions with participation of La $5d$, Y $4d$, La $4f$ and Bi $6p$ electronic states are also shown. The inserts show total densities of states according to the calculated data in [37].

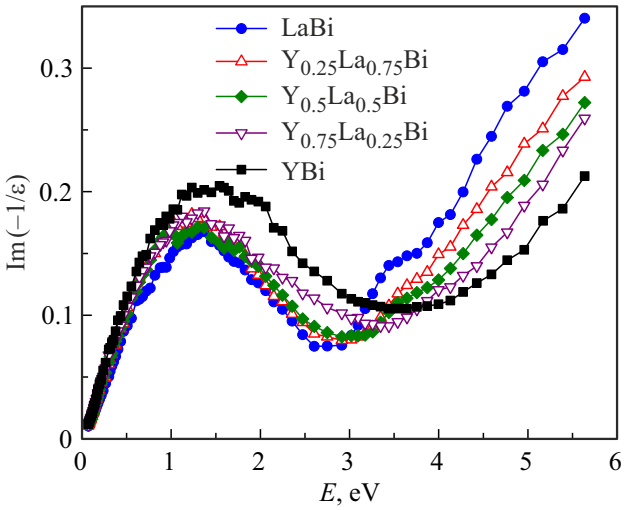

Figure 4. Volumetric characteristic electron energy loss functions of $Y_xLa_{1-x}Bi$.

units together with the empirical dependences in Figure 2. Comparison shows qualitative agreement between the theoretical and experimental curves. Both for binary and ternary compounds, the calculations reproduce the main features and transformation behavior of the spectra when the impurity content increases. In particular, the calculation adequately describes localization and width, profile variation and shit in energy of the main absorption band that occurs as x varies.

Let us address in detail the origin of wide absorption bands in $\sigma(E)$ spectra on the example of binary intermetallic YBi and LaBi and $Y_{0.5}La_{0.5}Bi$ with intermediate composition. According to the densities of electronic states shown according to [37] in inserts in Figure 3, the origin of intensive interband absorption is similar in these materials. It is primarily associated with quantum transitions of electrons from filled hybridized Y $4d$, $5p$ (La $5d$, $6p$) and Bi $6p$-bands to free Y $4d$ (La $5d$, $4f$) energy bands. The corresponding bands are identified with the high value ranges of $N(E)$ that have various structures and are separated from each other by a deep gap. Figure 3 shows, together with interband optical conductivities calculated from full densities $N(E)$, the most significant contributions associated with various electronic states. Thus, in binary YBi the main contribution to the formation of absorption band is caused by electronic excitations with participation of Y $4d$ and Bi $6p$-bands. Such transitions form two wide bands with peaks near 4.3 eV. In LaBi and $Y_{0.5}La_{0.5}Bi$, in turn, as follows from the structures of partial contributions, peaks in $\sigma(E)$ are caused mainly by electron transitions from filled states below E_F to free $4f$-states. Absorption bands formed by such transitions have an asymmetrical form with a „bulge" on the high-energy slope. Thus, frequency dispersion of the optical conductivity spectra of $Y_xLa_{1-x}Bi$ features mainly the presence of high interband light absorption at energies higher than ~ 1 eV and an abnormally low low-energy contribution. The structure of $\sigma(E)$ is qualitatively interpreted by calculations of the band structure of these materials [37] that predicted wide (~ 2 eV) gaps at the Fermi level in the densities of electronic states and indicates their semimetallic properties.

The complex permittivity components ε_1 and ε_2 obtained experimentally allow the volumetric electron energy loss functions $\mathrm{Im}(-1/\varepsilon) = \varepsilon_2/(\varepsilon_1^2 + \varepsilon_2^2)$ to be calculated for all compounds. This parameter whose peak occurs at $\varepsilon_1 \to 0$ describes discrete electron loss in volumetric plasma oscillation excitation. Position of the function peak on the energy scale is used to estimate the plasma frequency of conduction electrons. Energy dependences $\mathrm{Im}(-1/\varepsilon)$ shown in Figure 4 indicate that such peaks are localized of all compounds near 1.4 eV, that corresponds to the plasma frequency equal to $\omega_p = 1.8 \cdot 10^{-15}\,\mathrm{s}^{-1}$.

4. Conclusion

Optical properties of a family of semimetallic $Y_xLa_{1-x}Bi$ ($0 \le x \le 1$) with cubic crystalline structure have been studied in a wide wavelength range, including IR, visible and UV bands. Using the ellipsometric method, frequency dependences of dielectric functions, optical conductivity, reflectivity and electron energy loss were measured. It has been shown that the behavior of optical conductivity frequency dispersion in the main band of interband absorption and the main structural features were satisfactorily described using previous ab initio band calculations of these compounds [37]. Abnormally low values of $\sigma(E)$ in the long-wavelength band observed for all materials also correlate with these calculations that have shown the presence of wide gaps at E_F in the densities of electronic states.

Funding

The study was carried out under the state assignment of the Ministry of Education and Science of the Russian Federation (topic „Electron", No. 122021000039-4).

Conflict of interest

The authors declare that they have no conflict of interest.

References

[1] C.-G. Duan, R.F. Sabirianov, W.N. Mei, P.A. Dowben, S.S. Jaswal, E.Y. Tsymbal. J. Phys.: Condens. Matter **19**, *31*, 315220 (2007).
[2] O. Vogt, K. Mattenberger. Handbook on the Phisics and Chemistry of Rare Earth. Ch. 114. Magnetic measurements on rare earth and actinide monopnictides and monochalcogenides / Ed. K.A. Gschnedner, L. Eyring, G.H. Lander, G.P. Chopping. Elsevier Sci. Publ. (1993). V. 17. P. 301–407.
[3] D.X. Li, Y. Haga, H. Shida, T. Suzuki, Y.S. Kwon, G. Kido. J. Phys.: Condens. Matter **9**, *48*, 10777 (1997).

[4] P. Pandit, V. Srivastava, M. Rajagopalan, S.P. Sanyal. Physica B: Condens. Matter **405**, *9*, 2245 (2010).
[5] A.K. Sahu, A. Singh, P.K. Jha, S.P. Sanyal. Phase Transitions: Multinational J. **84**, *7*, 603 (2011).
[6] A. Louafi, Y. Chaouche, A. El Hassasna. Appl. Phys. A **127**, 506 (2021).
[7] P. Ruszała, M.J. Winiarski, M. Samsel-Czekała. J. Phys. Chem. Solids **159**, 110274 (2021).
[8] D.X. Li, Y. Haga, H. Shida, T. Suzuki. J. Appl. Phys. **80**, *1*, 264 (1996).
[9] D.X. Li, Y. Haga, H. Shida, T. Suzuki, T. Koide, G. Kido. Phys. Rev. B **53**, *13*, 8473 (1996).
[10] M.P. Volkov, N.N. Stepanov. Phys. Solid State **61**, *8*, 1416 (2019).
[11] L. Ye, T. Suzuki, C.R. Wicker, J.G. Checkelsky. Phys. Rev. B **97**, *8*, 081108(R) (2018).
[12] M. Zhang, X. Wang, A. Rahman, R. Dai, Z. Wang, Z. Zhang. Phys. Rev. B **101**, *6*, 064106 (2020).
[13] E.J.R. Plaza, C.S. Alves, A.A. Coelho, S. Gama, P.J. von Ranke. J. Magn. Magn. Mater. **272–276**, *3*, 2373 (2004).
[14] R. Pittini, J. Schoenes, O. Vogt, P. Wachter. Phys. Rev. Lett. **77**, *5*, 944 (1996).
[15] D.B. Ghosh, M. De, S.K. De. Phys. Rev. B **67**, *3*, 035118 (2003).
[16] P. Kumari, D.S. Yadav. J. Pure Appl. Industr. Phys. **8**, *5*, 54 (2018).
[17] E.M. Krivoy, A.P. Vasudev, S. Rahimi, R.A. Synowicki, K.M. McNicholas, D.J. Ironside, R. Salas, G. Kelp, D. Jung, H.P. Nair, G. Shvets, D. Akinwande, M.L. Lee, M.L. Brongersma, S.R. Bank. ACS Photonics **5**, *8*, 3051 (2018).
[18] N. Acharia, S.P. Sanyal. Solid State Commun. **266**, 39 (2017).
[19] G. Vaitheeswaran, V. Kanchana, M. Rajagopalan. Physica B: Condens. Matter **315**, *1–3*, 64 (2002).
[20] O. Pavlosiuk, P. Swatek, D. Kaczorowski, P. Wiśniewski. Phys. Rev. B **97**, *23*, 235132 (2018).
[21] F.F. Tafti, M.S. Torikachvili, R.L. Stillwell, B. Baer, E. Stavrou, S.T. Weir, Y.K. Vohra, H.-Y. Yang, E.F. McDonnell, S.K. Kushwaha, Q.D. Gibson, R.J. Cava, J.R. Jeffries. Phys. Rev. B **95**, *1*, 014507 (2017).
[22] C.Q. Xu, B. Li, M.R. van Delft, W.H. Jiao, W. Zhou, B. Qian, N.D. Zhigadlo, D. Qian, R. Sankar, N.E. Hussey, X. Xu. Phys. Rev. B **99**, *2*, 024110 (2019).
[23] B. Qian, F. Tang, Y.R. Ruan, Y. Fang, Z.D. Han, X.F. Jiang, J.-M. Zhang, S.Y. Chen, D.H. Wang. J. Mater. Chem. C **6**, *37*, 10020 (2018).
[24] M. Shoaib, G. Murtaza, R. Khenata, M. Farooq, R. Ali. Comput. Mater. Sci. **79**, 239 (2013).
[25] M. Kakihana, K. Nishimura, T. Takeuchi, Y. Haga, H. Harima, M. Hedo, T. Nakama, Y. Onuki. J. Phys. Soc. Jpn. **88**, *4*, 044712 (2019).
[26] Z. Charifi, A.H. Reshak, H. Baaziz. Solid State Commun. **148**, *3–4*, 139 (2008).
[27] S. Cui, W. Feng, H. Hu, Z. Feng, H. Liu. Solid State Commun. **149**, *25–26*, 996 (2009).
[28] S. Azzi, H. Boublenza, A. Zaoui, M. Ferhat. Comput. Mater. Sci. **65**, 331 (2012).
[29] A.K. Ahirwar, M. Aynyas, Y.S. Panwar, S.P. Sanyal. Adv. Mater. Res. **1141**, 39 (2016).
[30] F. Driss Khodja, A. Boudali, K. Amara, B. Amrani, A. Kadoun, B. Abbar. Physica B: Condens. Matter **403**, *23–24*, 4305 (2008).
[31] Y.O. Ciftci, K. Colakoglu, E. Deligoz. J. Phys.: Condens. Matter **20**, *34*, 345202 (2008).
[32] M. Narimani, Z. Nourbakhsh. J. Phys. Chem. Solids **145**, 109537 (2020).
[33] Nisha, H.S. Saini, N. Kumar, S. Singhmar, J. Thakur, S. Srivastava, M.K. Kashyap, A.H. Reshak. Phys. Lett. A **384**, *31*, 126789 (2020).
[34] Y. Wu, T. Kong, L.-L. Wang, D.D. Johnson, D. Mou, L. Huang, B. Schrunk, S.L. Bud'ko, P.C. Canfield, A. Kaminski. Phys. Rev. B **94**, *8*, 081108(R) (2016).
[35] N. Kumar, C. Shekhar, J. Klotz, J. Wosnitza, C. Felser. Phys. Rev. B **96**, *16*, 161103(R) (2017).
[36] B.H. Yu, Z.Y. Tian, F. Sun, D.C. Peets, X.D. Bai, D.L. Feng, J. Zhao. Opt. Express **28**, *11*, 15855 (2020).
[37] M.E.A. Belhadj, H. Rached, D. Rached, S. Amari. Comput. Condens. Matter **16**, e00295 (2018).
[38] P. Wadhwa, T.J.D. Kumar, A. Shukla, R. Kumar. Solid State Commun. **358**, 114976 (2022).
[39] M.A. Ordal, L.L. Long, R.J. Bell, S.E. Bell, R.R. Bell, R.W. Alexander Jr., C.A. Ward. Appl. Opt. **22**, *7*, 1099 (1983).
[40] Yu.V. Knyazev, A.V. Lukoyanov, Yu.I. Kuz'min. Opt. Mater. **129**, 112466 (2022).
[41] Yu.V. Knyazev, Yu.I. Kuz'min, S.T. Baidak, A.V. Lukoyanov. Solid State Sci. **136**, 107085 (2023).
[42] I.A. Nekrasov, Yu.V. Knyazev, Yu.I. Kuz'min, A.G. Kuchin, V.I. Anisimov. Phys. Met. Metallography **97**, *2*, 129 (2004).

Translated by E.Ilinskaya